Interfacial Dipole Formation and Surface-Electron Confinement in Low-Coverage Self-Assembled Thiol Layers: Thiophenol and *p*-Fluorothiophenol on Cu(111)

Sung-Young Hong,[†] Po-Chun Yeh,[‡] Jerry I. Dadap,[§] and Richard. M. Osgood, Jr.[§,*]

[†]Department of Chemistry, [‡]Interdepartmental Program in Solid State Science and Engineering, [§]Department of Applied Physics and Applied Mathematics, Columbia University, New York, New York 10027, United States

ABSTRACT Model systems of organic self-assembled monolayers are important in achieving full atomic-scale understanding of molecular-electronic interfaces as well as the details of their charge transfer physics. Here we use two-photon photoemission to measure the evolving unoccupied and occupied interfacial electronic structure of two thiolate species, thiophenol and *p*-fluorothiophenol, adsorbed on Cu(111) as a function of molecular coverage. Our measurements focus on the role of adsorbates in shifting surface polarization and effecting surface electron confinement. As the coverage of each molecule increases, their photoemission-measured work functions exhibit nearly identical behavior up to 0.4—0.5 ML, at which point their behavior diverges; this behavior can be fit to an interfacial bond model for the surface dipole. In addition, our results show the emergence of an interfacial electronic state 0.1—0.2 eV below the Fermi level. This electronic state is attributed to quantum-mechanical-confinement shifting of the Cu(111) surface state by the molecular adsorbates.

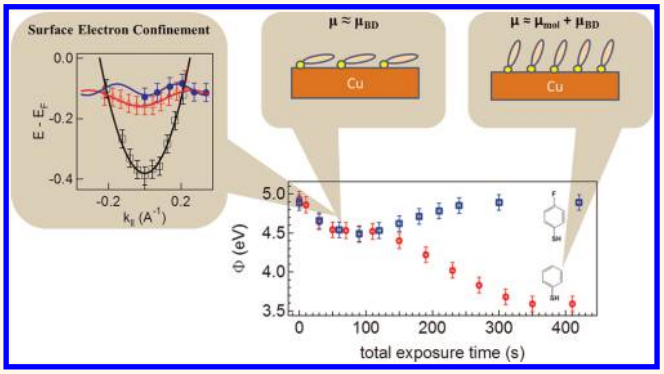

KEYWORDS: self-assembled monolayer · interfacial dipole · electron confinement · thiophenol · two-photon photoemission · Cu (111)

Organic-materials-based electronics are of increasing interest because this materials system can be lightweight, thin, flexible and can exhibit new functionalities.[1] In most cases understanding interfacial electronic structure is a key factor in solving many of the chemical and electronic issues[1,2] in these devices; it also gives rise to a series of important fundamental questions,[1−6] including the nature of interface polarization, the height and thickness of interfacial energy barriers and level alignment, interfacial molecular control and its chemical state, interfacial abruptness, and local charge density. These experiments have used samples prepared under either ambient or ultrahigh vacuum (UHV) conditions. UHV conditions enable the use of high resolution proximal and electron spectroscopies, as well as highly characterized initial substrate surfaces.

Thus, thiols, in particular, have been of interest to the organic electronics community both as a model molecular class as well as being useful for a series of practical applications including tunable nanoscale contacts and controllable thin film morphologies and interfaces.[3,7] In some cases, thiols interact with the surface and other adsorbates, either with or without the loss of hydrogen at the headgroup, to form a self-assembled monolayer (SAM) of the intact thiol or as thiolates, respectively, on a variety of surfaces.[7−13] In addition, the selection of thiol functional groups is useful for work function tuning.[3]

Thiol films or layers have a coverage-dependent phase transition.[14] Thus at low coverage, the film structure is loosely packed

* Address correspondence to osgood@columbia.edu.

Received for review August 15, 2012 and accepted November 14, 2012.

Published online 10.1021/nn303715d

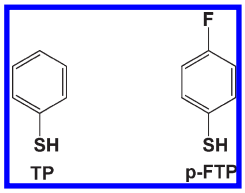

Figure 1. Thiophenol (TP) and *p*-fluorothiophoenol (*p*-FTP).

and in a supine or "lying-down" geometry, while at high coverage, a phase transition occurs and the film structure becomes densely packed with the molecules adopting a "standing-up" geometry. This structural difference has, in fact, been shown to change the work function and electronic structure of thin films structure, on which the thiol has adsorbed.[15−18]

One class of thiols, which has received much attention, is that of aromatic thiols. These materials can be organic semiconductors, which allow close chemical contact with a substrate. Their high conductivities have been verified by single-molecule transport measurements and density functional theory (DFT) studies.[19] These results are consistent with reports demonstrating that organic field effect transistors, whose electrodes are treated by aromatic thiols, have better performance than the ones treated by alkanethiols.[20] In addition, recent scanning tunneling microscopy (STM) studies showed that selection of chemical moiety and control of surface density can lead to the formation of patterned islands or layers on metal surfaces.[21−23] This surface patterning has potential applications in molecular electronics and gas sensing.

In this paper, we use two-photon photoemission (TPPE) to make a comparative examination of thiophenol and *p*-fluorothiophenol (see Figure 1) adsorbed on a Cu(111) surface as a function of coverage, that is, 0−1 ML, with emphasis on values less than ∼0.5 ML. Characterization of the adsorbed layers of each of these molecules on Cu(111) dosed under UHV conditions has been reported in the literature for STM and X-ray photoemission spectroscopy (XPS) probes.[23,24] The central difference between the two molecules is that in the latter, the para-positioned hydrogen is replaced by fluorine. This replacement leads to nearly opposite dipole orientations but with comparable magnitudes, that is, $|\mu_0|$ = 1.24 D for thiophenol (TP) and $|\mu_0|$ = 1.11 D for 4-fluorothiophenol (*p*-FTP), based on MP2 calculations.[25] Thus the dipole of thiophenol points away from the thiol group but that of 4-fluorothiophenol points toward it. In our paper, we use gas dosing within a UHV system to deposit thiol films of controllable coverage on a Cu(111) surface at room temperature. Our TPPE experiments measure a marked difference in the interfacial dipoles of the two molecules and show how the interaction of the adsorbed molecule with the surface electron leads to a new electronic-state structure due to confinement of the surface electron and, in addition, we are able to observe

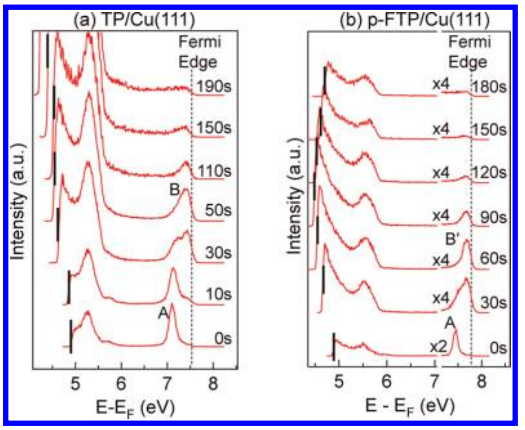

Figure 2. TPPE spectra of (a) TP/Cu(111) and (b) *p*-FTP/Cu(111) at low coverage. These series of spectra were collected at different exposure times shown in the right side of each figure. The photon energies used are 3.76 and 3.88 eV for TP and *p*-FTP, respectively. At the bottom of each panel, the TPPE spectrum of clean Cu(111) is shown. Each thick solid line indicates the low-energy cutoff for each photoemission spectrum. The Fermi edge is also indicated as a dashed line. Features A (surface state), B and B′ (new features) have binding energies of ∼0.4, 0.16, and 0.14 eV, respectively. The details of the data are explained in the text.

the consequences of this change in the molecular orientation, hence, surface polarization, as a function of coverage.

RESULTS

TPPE Spectroscopy at low coverage of TP and *p*-FTP. Our experiment consisted of exposing a bare surface to a calibrated dose of either of the two molecular species. The TPPE electron energy distribution curve (EDC) was then recorded at different photon energies. Each measurement consisted of ∼1 s of exposure at a specific angle setting. Care was taken to ensure that the adsorbate surface was not photochemically altered during the irradiation period by the UV laser.

A representative set of data, taken at normal emission angle and $E_{h\nu}$ = 3.76 eV (TP) and 3.88 eV (*p*-FTP) for a series of doses, where $E_{h\nu}$ is the photon energy, is shown in Figure 2. Prior to any exposure, measurements were made on the pristine Cu(111) surface, which in each case exhibited a sharp low-energy electron diffraction (LEED) pattern. As seen in Feature A, on the clean surface, an EDC from a clearly resolved Shockley surface state was obtained at the well-known binding energy of ∼0.4 eV.[26] When the surface was exposed to TP, the signal from the Shockley surface state decreased with each increasing exposure and a new state, labeled B, grew with the coverage. This peak was located at an energy −0.16 eV with respect to the Fermi level. In addition, as the exposure increased, the low-kinetic-energy cutoff decreased in energy monotonically; this decrease originates from a decrease in the surface work function, as will be discussed below. Also note that as the exposure increased to beyond

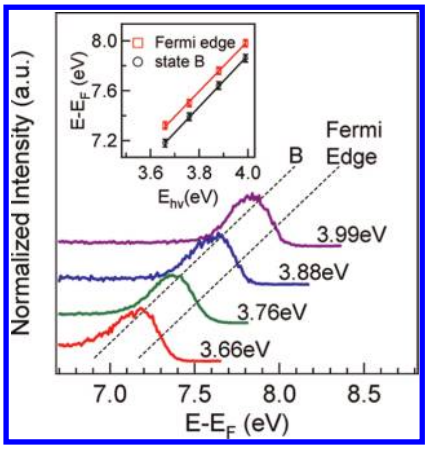

Figure 3. TPPE spectra of TP/Cu(111) with different photon energies ($E_{h\nu}$ = 3.66−3.99 eV). Dashed lines indicate shifts of peak B (left) and the Fermi level (right). The amount of peak shift is, to within error, $2\Delta E_{h\nu}$, as shown in the inset.

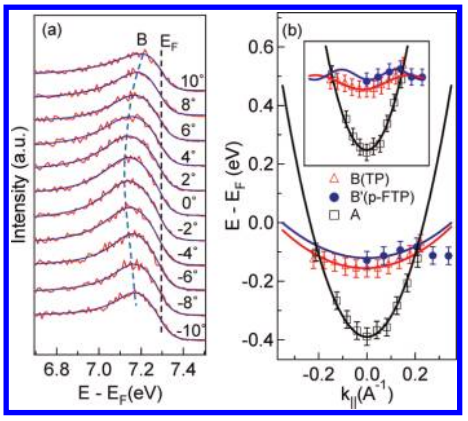

Figure 4. (a) Angle-resolved TPPE spectra around peak B with $E_{h\nu}$ = 3.65 eV. The detector angle is shown on the right side. The dashed blue and black guide lines indicate peak B and the Fermi edge, respectively. (b) The dispersion curves of peak B for TP and *p*-FTP. Also the dispersion of surface state (A) on the bare surface is also shown for comparison. The photoelectron parallel momenta in the *x*-axis are obtained from the measured detector angle using eq 3. The inset shows a periodic potential fit for peaks B and B′. The data were collected at an exposure time of 150 s for TP and 60 s for *p*-FTP, respectively.

50 s, state B decreased in amplitude. Finally low-coverage data were also taken for *p*-FTP and a similar new state located at −0.14 eV appeared and grew as the coverage increased. However, note that for the *p*-FTP data shown in Figure 2, the decrease in the low energy cutoff and the increase in the corresponding secondary (low energy threshold) electron counts ceased for an exposure above ∼90 s; after that exposure, the cutoff then increased and the corresponding secondary electron signal decreased as the exposure was further increased.

As described in the Experimental Section, our use of TPPE permits the identification of the origin of a spectral feature as being either in the initial, intermediate, or final state of the TPPE process by means of a measurement of the electron energy given by $E = E_k + \Phi + E_F$ *versus* the photon energy $E_{h\nu}$, where E_k is the photoelectron kinetic energy, E_F is the Fermi level, and Φ is the work function. In particular, the slope of the shift in the peak of a spectral feature *versus* photon energy, that is, $dE/dE_{h\nu}$, is used to determine the nature of the feature. For example, prior measurements have shown $dE/dE_{h\nu} = 2$ from the clean Cu(111) surface state because this state lies below the Fermi level. Figure 3 shows such a measurement for the case of the −0.16 eV peak using TPPE with $E_{h\nu}$ = 3.66, 3.76, 3.88, and 3.99 eV. Thus in this case the measurement also showed a slope of 2 indicating that the peak is associated with an occupied state.

Angle-Resolved Measurements of Spectra. The angle-resolved capability of the TPPE system was also used to determine the dispersion, that is, *E versus* $k_{\|}$ of the features B (TP) and B′ (*p*-FTP). The results from this measurement for TP are shown in the data of Figure 4a. This measurement was done at an exposure time of 140 s to minimize the contribution of the bare Cu surface state, that is, at a coverage for which the bare surface state is fully extinguished. Angle-resolved photoemission spectra were also measured for *p*-FTP (not shown here, see Supporting Information) at lower exposure time (60 s). Also shown in Figure 4b are basic fits to the data based on the assumption that it has a parabolic dependence of *E versus* $k_{\|}$; the fits showed an effective mass of $m^* \approx 3.5 \pm 0.5\ m_e$ for TP and $3.9 \pm 1.4\ m_e$ for *p*-FTP, where m_e is the electron mass. Clearly this effective mass is much greater than that of the surface state ($m^* = 0.5 \pm 0.1\ m_e$) of bare Cu(111) as shown in Figure 4. Note however, that this parabolic fit is less satisfactory for the data at larger values of $k_{\|}$. In fact a better fit is obtained if a simple harmonic dependence is assumed for the dispersion as shown in the inset of Figure 4b. This fit suggests that there is backfolding of this occupied state at $k_{\|} > 0.2$ Å^{-1}. This important point will be discussed below. Recently, similar backfolding behavior was also seen for a periodic coupled quantum well structure or superlattice for Cu(111) covered by a periodic adsorbate-molecule structure.[27] In that prior work, it was concluded that the adsorbate molecules localized the surface electrons.

TPPE Spectroscopy of TP at High Coverage. The goal of this paper is to examine the *low-coverage* comparative behavior of our two benzene thiols, which have opposite dipole orientation. However, since there has been one previous report[28] of the TPPE spectra of TP on a Cu(111) surface *at high coverage*, we made an initial measurement of this spectra of this system at high exposure so as to provide useful cross check on the consistency of our system with that of ref 28. Our measurement was made at a photon energy of 3.76 eV, since it was relatively close to that used in the reference, and employed a series of exposures equal to or longer than 150 s (see Figure 5). Note also this high-coverage data shows no traces of the features (discussed above)

observed at low-coverage. The most prominent and best defined feature in the data is a peak at 6.75 eV above the Fermi level, although a smaller feature is also noticeable at 6.91 eV (see the inset of Figure 5). The absolute energy and separation of the 6.75 and 6.91 eV peaks are very close to those in ref 28. Finally, based on the measurements of kinetic energy vs photon energy by us and ref 28, these two observed states are assigned to a final state at 6.75 eV and an intermediate state at 3.16 eV, respectively.

Note that while these states are of interest here as an important consistency check with earlier measurements in ref 28, their assignments are of interest in their own right. Thus, ref 28 revealed that both states appear to exhibit σ symmetry and their energetic locations are nearly independent of the length of hydrocarbon chain. The origins of both states were initially attributed to σ^*_{CuS} and a combination of σ^*_{CS} and π^*_{CuS} based on *ab initio* simulations;[28] however, this assignment has apparently come into question as a result of other photoemission studies, which found another unoccupied state at 1.2−1.6 eV that was attributed to an atomic S or thiol/metal interface bond.[16,29−31] Those studies also suggest that there may well be a similar unoccupied state at the TP/Cu(111) interface even though we cannot discern it because the state is imbedded in an energy range filled with secondary electrons. Careful spectroscopic measurements are desirable to clarify the existence of an unoccupied state at a lower-energy level. Also we want to point out another possible origin of the 3.16 eV feature rather than that of a molecular state. Recent TPPE studies on alkanethiol/Au(111) found an image-like interface state below the vacuum level.[32] This state was also found to be independent of the hydrocarbon group as well. Its effective mass was found to be close to the free-electron mass, and ref 28 also reported that 3.16 eV is dispersive even though the data are not shown in the paper. Thus, further experimental and theoretical studies are necessary to fully understand the origin of this state.

Note that in addition to these unoccupied states, we observed another final state at ~6.13 eV above the Fermi level. Using the measurements of kinetic energy *versus* photon energy data, we confirmed that this state is an occupied state with a binding energy of 1.4 eV. This state is known to arise from an antibonding orbital of the Cu−S bond; see, for example, the case of S/Cu(100)[31] and the case of methanethiol/Cu(100)[33] both at similar energies.

DISCUSSION

Prior Work on Thiols on Cu(111) or Related Cu Surfaces. Because of the importance of thiols in forming prototypical self-assembled monolayers, there have been extensive experimental and theoretical studies probing

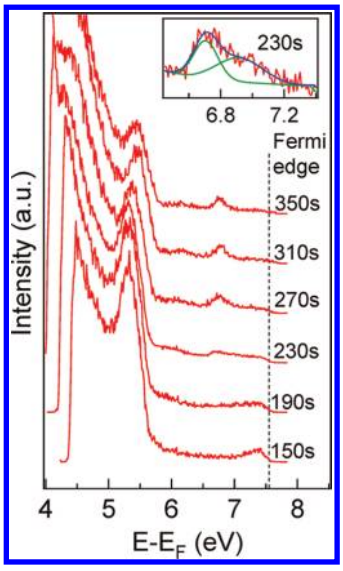

Figure 5. TPPE spectra on TP/Cu(111) at a series of high coverage values of adsorbate molecules taken at a photon energy of 3.76 eV. This series of spectra were collected for the different exposure times shown on the right side of the panel. The dashed line indicates the Fermi edge. The inset shows a two-peak fitting of the spectrum taken at an exposure time of 230 s.

the detailed interfacial chemistry of these molecules, adsorbed on Cu surfaces.[11,13,18,22−25,28,31,33−37] For example, in the case of TP and *p*-FTP, near-edge X-ray absorption fine structure (NEXAFS) studies of those molecules on Cu(100) surface revealed that the tilt angles of TP and *p*-FTP were 21° and 25° from the surface normal for 1 ML coverage, respectively.[25] For TP/Cu(111), earlier angle-resolved ultraviolet photoemission spectroscopy (UPS) studies showed that the orientation of TP was perpendicular or nearly perpendicular at full coverage.[24] By comparison, more recent detailed studies of the surface structure of TP and *p*-FTP were conducted by Wong, *et al.*[23] They used low-temperature STM and DFT to reveal the lattice structure and orientation of TP, *p*-FTP, and other halogenated TPs on Cu (111). In particular, they found that when the coverage was sufficiently low, for example, at 0.25 ML, TP was found to lie in a flat geometry, whereas at ~1 ML it was aligned vertically. In particular, the tilt angle of TP was 65° from the surface normal at low coverage. This same group also showed that the lateral interaction of halogenated TPs led to a different self-assembled structure at low coverage. In addition, other DFT studies for TP monolayers on Cu(111) showed that the tilt angle was along the surface normal.[36]

In contrast to the more numerous chemical and surface-structure studies of intact TP and other thiols on Cu(111), there are fewer studies of the electronic structure at <1 ML and the coverage dependence and electronic-state assignment appears not to have been examined. Thus, Vondrak *et al.* used TPPE to examine the unoccupied-state structure of a full monolayer of

TP plus other alkanethiols on Cu(111).[28] Their measurements of the TP surface were carried out under full-coverage conditions and are discussed in more detail below. While electronic-structure studies with benzenethiols have not been extensive, there have been several measurements, which have observed the electronic structure and coverage-dependent shifts of benzene[38−40] and other organic species including strongly periodic systems on Cu(111)[27] and other metals.[41−43] Of particular interest have been observation of low-coverage shifts of the Cu(111) surface state[39] and image states[38] upon adsorption of these species. In addition, as mentioned above, strong backfolding was observed for an adsorbate system having a periodic surface arrangement.[27] These observations are commented on in more detail below.

Work Function Variation with Coverage. One of our most striking observations is the strong change in the low-energy cutoff with coverage that is observed for both TP and *p*-FTP at low coverage as shown in Figure 2, as well as the fact that this behavior occurs with opposite polarity for each of the two molecules. This shift in low-energy cutoff can be related to a more fundamental quantity, the change in work function, by using the fact that for TPPE, the work function is given by $\Phi = 2h\nu - (E_F - E_{LC})$, where E_F and E_{LC} are the Fermi edge and the low-energy cutoff in the TPPE spectra, respectively.[17,44]

Using the above relation, we plot the coverage-dependence of the work function for surfaces covered with one of the two different molecules as a function of exposure in Figure 6a. The horizontal axis is the exposure time of the molecules. In addition to this axis, we have provided an auxiliary scale showing the approximate coverage obtained with this exposure. Use of the data in ref 23 allows us to calibrate the curve of work function *versus* exposure. In particular this and other studies by the same group showed that upon adsorption at low-coverage, *p*-FTP initially forms a loosely packed honeycomb structure of face-down molecules. However a further increase in coverage leads to a denser structure with higher coverage of the face-down phase. The observations for the second or denser "lying-down" phase and our measurements of the coverage dependence of the work function allow us to estimate the coverage using a plot based on the first-order adsorption kinetics. Our estimation of coverage relies on the assumption that the work function is proportional to coverage. This assumption is valid only for low coverage because depolarization effects, which result in a sublinear dependence with coverage, are then much less pronounced as has recently been shown, for example, by the Monti Group.[6] (Calculations are presented in the Supporting Information.) For both molecules, the change of work function with coverage is nearly identical at up to 0.4−0.5 ML. At this point, both systems exhibit an inflection point in their coverage-*vs*-work-function

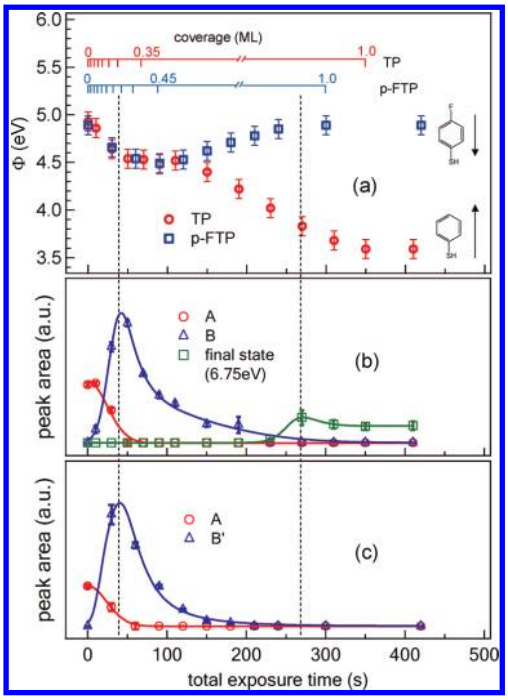

Figure 6. (a) Measured work function as a function of the total exposure time of TP (red circle) and *p*-FTP (blue square) on Cu(111). Auxiliary scales at the top of the figure show the approximate coverage for a given exposure. The inflection point of both curves appears at ∼100 s. The plateau at ∼270 s indicates the saturation of the coverage of the adsorbed molecules on the substrate. TP and *p*-FTP are drawn as an inset with arrows indicating the dipole projected along the 1−4 molecular axis. (b,c) The peak areas of the surface state (A, red circle), the new feature (B or B′, blue triangle), and the final state at 6.75 eV (green square) as a function of total exposure time of TP (b) and *p*-FTP (c) on Cu(111). The data points for each state were connected by a guide to the eyes for better visibility. The dashed lines were drawn to indicate the alignment of similar features between graphs.

plot and then diverge with slopes of opposite polarity as the coverage further increases. Note that near the inflection point (50−110 s) for the TP and the *p*-FTP curves, the slope of the graph is close to zero.

These observations regarding work function change can be understood by considering a simple model used in a recent study of benzenethiols on a Cu(100) surface, which examined how these and other loosely related molecules alter the work function of the Cu surface.[25] A similar approach has also been applied in other studies using alkanethiol and fluoroalkanethiols.[45,46] In this approach, the molecular component of the overall surface work function is approximated as having a contribution from the projected molecular dipole onto the surface normal plus a dipole polarization due to the molecular bond. This molecular bond dipole includes charge redistribution, a "push-back" effect due to Pauli repulsion, and other possible effects upon formation of a chemisorbed bond by the adsorbate. As with other groups who have employed this simple description, we do not take into account the electrostatic interaction

between the dipoles, which may reduce (depolarize) the effective dipole moment per molecule at higher coverage.[47] In the case of TP and other thiols, STM studies have shown that at low coverage, these molecules are known to have a supine or lying-down geometry and thus their dipole projection normal to the surface is then very small and at low coverage the bond-dipole contribution is then dominant. However, as the coverage increases, the adsorbate begins to assume its standing-up phase; thus at high coverage the molecular dipole contribution becomes important.

Hence, the behavior in Figure 6 is related to the phase transition from a supine to a standing-up orientation. If the orientation of the two molecules was not fully supine, the two curves would not be coincidental in the first part of the curve, since for a supine molecule there is no molecular component perpendicular to the surface and thus the work function depends chiefly on the bond dipole. Since the work function change in this region is proportional to the product of the molecular density and the bond dipole moment, the work function change slows as the coverage saturates for near full coverage of molecules, which are oriented in the supine position. At this point in coverage, molecules then change their orientation to the vertical orientation and the surface concentration can then increase further. Note that as pointed out by others, this process is known to involve surface domains rather than individual molecules.[23] Subsequently, domains with standing-up conformation increase as the surface concentration of molecules also increases. In fact, prior STM studies showed the mixed-domain structure of standing-up and supine benzenethiols. After the inflection point, both curves begin to diverge, although the slope of the TP curve is a factor of ~1.6 times that of *p*-FTP. In this region of the curve, the slope is sensitive to the change in the total surface dipole as well as the increase in surface concentration. Since the bond dipole of *p*-FTP is antiparallel to the normal component of intrinsic molecular dipole, whereas that of TP is parallel, the total interface dipole consisting of these dipoles is smaller for *p*-FTP, thus making the slope for TP larger than that for *p*-FTP.

This simple model can be tested for quantitative internal consistency by using the known relationships between work function change and the two contributions to the surface dipole for each adsorbed molecule. In effect we obtain the total surface dipole/adsorbed molecule at 1 ML coverage and then extract out the dipolar contribution from the bond dipole/molecule, which to first order is not coverage dependent. This can then be used to predict the work function at the inflection point, that is, 0.4−0.5 ML, for which coverage the molecules are still dominantly in the supine position and thus the molecule contribution to the adsorbate dipole will be negligible. Thus based on the Helmholtz equation, the change in the work function at 1 ML can be related to the adsorbate surface coverage and the normal component of the total adsorbate dipole,

$$\Delta\Phi = -ne\mu_{\mathrm{ads},\perp}/\varepsilon_0 \quad (1)$$

where n is the surface density of the adsorbate dipoles and ε_0 is the vacuum permittivity; n can be derived from thiol studies on Cu(100). We use the value of n from known value for Cu(100) because the surface packing density of the erect thiols is governed by the thiol molecular size (see Supporting Information). Then using eq 1, the effective adsorbate polarization/adsorbate molecule is estimated to ~0.68 D and ~0 D for TP and *p*-FTP, respectively.

$$\mu_{\mathrm{ads},\perp} = \mu_{0,\perp}/\varepsilon_{\mathrm{eff}} + \mu_{\mathrm{BD}} \quad (2)$$

This equation has been used successfully for the case of benzenethiols on a Cu(100) surface.[25] The molecular dipoles, that is, $\mu_{0,\perp} = 0.97$ D and $\mu_{0,\perp} = -0.78$ D for TP and *p*-FTP, respectfully, are estimated from simulation data in ref 25 and orientation angles given in ref 37. We set $\varepsilon_{\mathrm{eff}} = 2.94$ for the two molecules, a reasonable assumption given that the molecules considered by us have the same polarizability as those in ref 25. Inserting $\mu_{\mathrm{ads},\perp}$ and $\mu_{0,\perp}$ into eq 2 for the two molecular species, we obtain a value of μ_{BD} for both molecular species of 0.31 D. Recalling that due to the supine molecule orientation at low coverage we can neglect the molecular dipole contribution, the work function change at the inflection point, with $n \approx 2 \times 10^{14}$ cm^{-2}, is then estimated using eq 1 to be *ca.* −0.23 to −0.28 eV; this value can be compared to our experimental value of ~ −0.4 eV.

The difference between the model calculation and experimental data can be attributed to the simplicity of the model used here, including the multiple assumptions for the model calculation, such as surface density of molecule, dielectric constant, tilt angle of benzene group, *etc.* One particularly important assumption in the model is that the bonding dipole is independent of coverage. This assumption may not be rigorously true. For example a recent theoretical study showed that the bond dipole of thiolate SAM is significantly affected by packing density even without taking into account a change in orientation.[47] In addition, since the benzene group is proximate to the surface at low coverage it will also to some extent influence the surface polarization.[38,40] This effect together with the electrostatic dipole−dipole interactions are obviously not accounted for in our model. *However while the model used here is approximate, it is clear that it does describe at least the dominant physics involved.*

Identification and Nature of the New State near −0.15 eV. The state located at a binding energy of 0.16 ± 0.08 eV is the most prominent low-binding-energy spectral feature of TP on Cu(111). Our measurement of the variation of kinetic energy with wavelength shows that it is an occupied initial

state. The same feature with the slightly different binding energy of 0.14 ± 0.04 eV was also measured in our experiments for adsorbed *p*-FTP. These two states appear not to have been commented on or even observed in any prior theoretical or experimental work: in fact, recent photon photoemission studies on thiol/Cu (or the closely related Au system) have found the highest occupied molecular orbital (HOMO) and lowest unoccupied molecular orbital (LUMO) levels located at less than −1 eV and greater than 1 eV from the Fermi level, respectively.[18,31,33,48−51] The additional distinctive characteristics of the −0.15 eV state are, first, that it is a spatially localized or very weakly dispersive state, as is shown *via* our angular-resolved measurements; this behavior is in contrast with the strongly dispersive nature of the usual clean Cu(111) surface state. Second its photoemission intensity is found to rise and then decrease with coverage over the range of 0−0.5 ML, that is, at low coverage. Examination of the data shows the appearance of this state is clearly associated with the deposition of TP on the surface, while its disappearance occurs after ∼0.4−0.5 ML, that is, the same coverage at which the TP begins to shift out of its supine position. The binding energy of this TP state (as well as, *mutatis mutandis*, its *p*-FTP analogue) is constant within experimental error at 0.1−0.3 ML coverage where this state is particularly prominent.

To identify this state, we consider two possible origins of the feature, including (1) a chemisorbed bond, which changes with surface phase or, more particularly, surface orientation or (2) a quantum-confined Cu surface state.

The first possible origin is that the state for either TP or *p*-FTP is a chemisorbed state that is quite apparent at low coverage, that is, at less than 0.4−0.5 ML. This low binding-energy state is not seen at coverage close to 1 ML (see Figure 2); a coverage which has been shown *via* STM studies[23] to be above that for which the molecule assumes a vertical geometry. Thus, this chemisorbed state would have to be identified with the supine orientation of the benzene thiols. Further note that no evidence of the state is seen at high, that is, ∼1 ML, coverage since the only states measured are, for TP, an unoccupied-state energy of 6.75 eV, and for *p*-FTP, an unoccupied state at 8.65 eV (not shown, see Supporting Information) for our data and data in ref 28, as well as an occupied state at −1.4 eV. Of course one must also consider if a change in surface phase, that is, molecular orientation in our case, could shift the binding energy of the 1.4 eV state to 0.16 eV between low and high coverage. However, there appears to have been no earlier examples of the change in S-metal surface bond energy with ligand orientation for thiols although there has been at least tentative observation for thiophene.[17] Moreover, our experiments show clear evidence that the −0.15 eV state originates from the Cu surface state rather than chemisorbed states between the Cu and adsorbate while the rise of the −0.15 eV state signal occurs simultaneously with a reduction in the surface state signal, whereas the three chemisorbed states just mentioned begin to show up after the −0.15 eV state becomes undetectable. This observation is consistent with the fact that −0.15 eV state was not observed in UPS studies of TP/Cu(100) system, for which the Shockley surface state is not present.[18] We thus conclude that it is unlikely that the −0.15 eV states would originate from any distinct, low-coverage, chemisorbed bond.

A more likely and experimentally consistent origin of the behavior of the −0.15 eV state and its behavior in Figures 2, 4, and 6 lies in the effect of new adsorbate molecules on the otherwise delocalized electron in the Cu(111) sp surface state. Such surface impurities can place lateral potential barriers throughout the surface, which can lead to confinement of the normally delocalized surface-state electron, and thus alter its binding energy. Such confinement shifts have been seen previously on surfaces having simple surface-structure-confined Cu(111) surface electrons.[52] For example, it is well-known that on regularly stepped Cu(111), prepared from a vicinal surface, binding-energy shifts in surface electrons are seen due to confinement of the electron by ∼10s of Angstrom-wide steps. Thus in ref 52, Wang *et al*. showed that with a simple 1-dimensional Kronig−Penney model, the surface-state energy shifts upward (decreasing binding energy) by about 200 meV as the terrace length decreased from infinite (flat surface) to ∼7.4 Å due to electron confinement. In addition, confinement effects have also been observed in a striped phase of O/Cu(110).[53]

In addition, and perhaps more to the point, there have been several prior studies of the confinement of the Cu(111) surface-state electron in the presence of adsorbate atoms or molecules. These studies include early theoretical work by Hormandinger and Pendry,[54] which developed a theoretical framework for adsorbate-induced surface-state-electron localization. This theoretical treatment related the confinement shift to the adsorbed-molecule-induced potential barriers. A more-recent *experimental* study used angle-resolved photoemission spectroscopy (ARPES) to show that a small, that is, 0.1 ML, addition of CO on the Cu(111) surface caused a decrease in the binding energy by 0.15 eV.[55] A second study, using benzene on Cu(111) along with a TPPE measurement, has shown a shift of the same magnitude.[39] Thus the shifts in these cases are typically within 100s of meV of the original bare-surface binding energy below the Fermi level, a magnitude close to the values measured in our coverage-dependent photoemission data shown in Figure 2. Finally, a third very relevant and elegant study used a 2D molecular surface lattice formed by adsorption of dehydrogenated 4,9-diaminoperylene-quinone-3,10-diimine onto a Cu(111) surface to demonstrate that a lateral surface superlattice

of the Cu surface electron could be formed.[27] The coupling within the superlattice was found to be weak thus yielding well-defined quantum wells. ARPES measurements showed a small electron dispersion and backfolding by the Brillouin zone of the surface lattice. The dispersion was fit by a near sinusoidal dispersion as would be expected by a periodic confinement potential.

In our TP- and *p*-FTP-dosed surface, the most substantial surface-molecule interaction would be *via* the S-metal bonding in adsorbate islands; in fact, some experiments have suggested that the benzene ring moieties are not in contact with the Cu surface[23] and thus would not present any substantial surface potential modulation. The S surface bond would be sufficiently disruptive that it is likely to form a surface barrier. In addition, these prior STM studies have shown that regular arrays of *p*-FTP are imaged on low coverage surfaces at 80 K.[23] In the case of TP-dosed surfaces, the molecular surface ordering is not as regular; nonetheless, STM imaging does show persistent patterns of centered hexagonal structures under closely related conditions. Our TPPE measurements are consistent with surface confinement by a regular array. Thus for both molecules, clear evidence for backfolding is seen in the angle-resolved measurement of the dispersion. Given the more pronounced surface ordering seen in *p*-FTP, it is not surprising that the adsorbate structure causes a larger energetic shift and stronger localization than does TP, as shown in Figure 4. Further note that the unit cell of 0.18 $Å^{-1}$ reported for *p*-FTP[17] agrees well with the backfolding wavenumber of 0.21 $\pm$ 0.03 $Å^{-1}$ seen in our data in Figure 4.

Thus our observed TPPE data are supportive of confinement being the source of the −0.15 eV state for TP and *p*-FTP. In particular, the fact that this spectral feature has the same spectral density as the unconfined electron state is consistent with a simple fixed confinement being the origin of this spectral feature. In addition, the fact that the new states show weak dispersion with a folded zone, which for the case of *p*-FTP is consistent with the known period, is also consistent with state being strongly confined.

Finally we note that it appears surprising that there is no signature of the final states, that is, those with energies of 6.75 and 6.91 eV *at low coverage*, which are only detected at exposures close to saturation; see Figure 6. While we do not have a definitive explanation of this observation, we note photoemission from molecules in a supine position or in a state of disorder might be expected to have a different, including much reduced, photoemission signature than those in an upright position. Clearly this phenomenon will require additional studies for a definitive answer.

CONCLUSIONS

The goal of our work has been to develop an understanding of how a low coverage of benzenethiols on Cu(111) affects electronic structure of the molecule–metal interface. Our first observation is that adsorption alters the surface polarization of the interfacial layer. Our results show that at low coverage the formation of an adsorbate metal bond provides the dominant source of polarization and as the coverage increases the change in adsorbate geometry to an upright geometry further shifts the surface dipole layer and hence the surface polarization. In addition, our results also show the importance of molecule-based surface confinement of the Cu surface electrons in altering their energetic location and dispersion of this surface band. The Umklapp features measured are in accord with earlier STM measurements of surface structure of these two adsorbates.

EXPERIMENTAL SECTION

Our experiments use a high-purity (99.999% purity) single-crystal Cu(111) sample of 1.2-cm diameter. The sample is placed in a UHV chamber (<2 × 10^{-9} Torr) equipped with an ion-sputtering gun, a low energy electron diffraction (LEED) instrument, a quadrupole mass spectrometer, and a spherical-sector electron-energy analyzer. The sample is prepared by Ar^+-sputtering at 1.5 keV for 20 min and subsequent annealing to 500 °C. Each sample preparation cycle is repeated until sharp LEED spots are observed. A UHV dosing system is used to prepare the molecule/Cu interface with its nozzle located 5 cm from the sample surface. A calibrated exposure of the surface is carried out by filling a known volume in the doser with a predetermined pressure of the thiol species; this calibrated reservoir is then opened to expose the sample. Thus all surface dosing is carried out on a clean surface in UHV and at room temperature. Further, surface exposure is carried out *via* additional dosing of the previously dosed surface. After each experimental run of ∼10 doses the surface is again cleaned and prepared by sputter annealing.

Our electronic structure and surface polarization experiments make use of angle-resolved TPPE. To obtain high signal-to-noise ratio while minimizing space-charge effects, our TPPE system uses a tunable ultrafast optical parametric amplifier driven by regeneratively amplified Ti:Sapphire laser pulses. The visible output pulses are then frequency-doubled in a nonlinear crystal, producing a train of wavelength-tunable UV, 90 fs pulses at 250 kHz repetition rate. The photon energies used ranged from ∼3.6 to 4 eV. The laser was focused on the sample at a typical maximum fluence of ∼10 $\mu J/cm^2$ and at a fixed incidence angle of 70°.

Photoemitted electrons are collected using a spherical-sector energy analyzer having a momentum resolution of $\delta k_{||}$ = 0.03 $Å^{-1}$ and the energy resolution set to ∼60 meV. The detector was rotated about the fixed sample so as to collect data along the $\bar{M}\bar{\Gamma}\bar{M}$ direction of the Cu(111) surface Brillouin zone. Our sample was biased at −4 V to reduce the effects of stray electric fields in the vicinity of sample. The resulting data were corrected for both the additional kinetic energy and change in the parallel momentum $k_{||}$ of the electrons due to this accelerating voltage using the method described in a literature.[26]

To discriminate between occupied and unoccupied states requires the measurement of a series of TPPE data, each with different photon energy at normal emission angle and the same surface properties. A comparison of the peak shift with photon energy allows determination of the nature of state being

examined. Thus for an occupied state, the peak shift is twice the photon-energy difference. For an intermediate state, the peak shift is equal to the photon-energy difference. For a final state, which is above vacuum level, there is no shift with a change in the photon energy. With regard to the angle-resolved capability, the measured angle θ of the detector and the measured kinetic energy E_k are related to the parallel momentum $k_{||}$ of the emitted electron *via* the well-known expression:

$$k_{||} = \frac{\sqrt{2m_e E_k}}{\hbar} \sin\theta \quad (3)$$

Note that a measurement of the dispersion curve of a specific spectral feature is well-known to allow determination of the degree of the localization of the state.

Finally we emphasize that our LEED observations of the bare surface together with our occupied-state photoemission capability enable us to fully characterize our UHV prepared Cu surface. In addition, our quadruple mass spectrometer (QMS) capability also enables full characterization of the adsorbate molecule prior to adsorption.

Conflict of Interest: The authors declare no competing financial interest.

Acknowledgment. We thank M. Hybertsen and L. Venkataraman for discussions and helpful suggestions regarding this experiment. This research is based solely upon work supported by the Center for Re-defining Photovoltaic Efficiency through Molecule Scale Control, an Energy Frontier Research Center funded by the U.S. Department of Energy, Office of Science, Office of Basic Energy Sciences under Award Number DESC0001085.

Supporting Information Available: Periodicity of *p*-FTP honeycomb structure, coverage estimation, photon energy dependence of TPPE spectra at full coverage TP and *p*-FTP, and notes on the dipole moments used here. This material is available free of charge *via* the Internet at http://pubs.acs.org.

REFERENCES AND NOTES

1. Koch, N. Organic Electronic Devices and Their Functional Interfaces. *ChemPhysChem* **2007**, *8*, 1438–1455.
2. Ishii, H.; Sugiyama, K.; Ito, E.; Seki, K. Energy Level Alignment and Interfacial Electronic Structures at Organic/Metal and Organic/Organic Interfaces. *Adv. Mater.* **1999**, *11*, 605–625.
3. Heimel, G.; Romaner, L.; Zojer, E.; Bredas, J.-L. The Interface Energetics of Self-Assembled Monolayers on Metals. *Acc. Chem. Res.* **2008**, *41*, 721–729.
4. Kahn, A.; Koch, N.; Gao, W. Electronic Structure and Electrical Properties of Interfaces between Metals and π-Conjugated Molecular Films. *J. Polym. Sci., Part B: Polym. Phys.* **2003**, *41*, 2529–2548.
5. L'vov, V. S.; Naaman, R.; Tiberkevich, V.; Vager, Z. Cooperative Effect in Electron Transfer between Metal Substrate and Organized Organic Layers. *Chem. Phys. Lett.* **2003**, *381*, 650–653.
6. Monti, O. L. A.; Steele, M. P. Influence of Electrostatic Fields on Molecular Electronic Structure: Insights for Interfacial Charge Transfer. *Phys. Chem. Chem. Phys.* **2010**, *12*, 12390–12400.
7. Love, J. C.; Estroff, L. A.; Kriebel, J. K.; Nuzzo, R. G.; Whitesides, G. M. Self-Assembled Monolayers of Thiolates on Metals as a Form of Nanotechnology. *Chem. Rev.* **2005**, *105*, 1103–1170.
8. Aqua, T.; Cohen, H.; Sinai, O.; Frydman, V.; Bendikov, T.; Krepel, D.; Hod, O.; Kronik, L.; Naaman, R. Role of Backbone Charge Rearrangement in the Bond-Dipole and Work Function of Molecular Monolayers. *J. Phys. Chem. C* **2011**, *115*, 24888–24892.
9. Camillone, N., III; Chidsey, C. E. D.; Liu, G.-y.; Scoles, G. Superlattice Structure at the Surface of a Monolayer of Octadecanethiol Self-Assembled on Au(111). *J. Chem. Phys.* **1993**, *98*, 3503–3511.
10. Camillone, III, N.; Khan, K. A.; Osgood, R. M., Jr The Thermal Chemistry of Model Organosulfur Compounds on Gallium Arsenide (110). *Surf. Sci.* **2000**, *453*, 83–102.
11. Jackson, G. J.; Woodruff, D. P.; Jones, R. G.; Singh, N. K.; Chan, A. S. Y.; Cowie, B. C. C.; Formoso, V. Following Local Adsorption Sites through a Surface Chemical Reaction: CH_3SH on Cu(111). *Phys. Rev. Lett.* **2000**, *84*, 119–122.
12. Nuzzo, R. G.; Zegarski, B. R.; Dubois, L. H. Fundamental Studies of the Chemisorption of Organosulfur Compounds on Gold (111). Implications For Molecular Self-Assembly on Gold Surfaces. *J. Am. Chem. Soc.* **1987**, *109*, 733–740.
13. Zhou, J.-G.; Williams, Q. L.; Hagelberg, F. CH_3SH Molecules Deposited on Cu(111) and Deprotonation. *Phys. Rev. B* **2008**, *77*, 035402.
14. Poirier, G. E.; Pylant, E. D. The Self-Assembly Mechanism of Alkanethiols on Au(111). *Science* **1996**, *272*, 1145–1148.
15. Lindstrom, C. D.; Muntwiler, M.; Zhu, X. Y. Electron Transport Across the Alkanethiol Self-Assembled Monolayer/Au(111) Interface: Role of the Chemical Anchor. *J. Phys. Chem. B* **2005**, *109*, 21492–21495.
16. Miller, A. D.; Gaffney, K. J.; Liu, S. H.; Szymanski, P.; Garrett-Roe, S.; Wong, C. M.; Harris, C. B. Evolution of a Two-Dimensional Band Structure at a Self-Assembling Interface. *J. Phys. Chem. A* **2002**, *106*, 7636–7638.
17. Zhou, J.; Yang, Y. X.; Liu, P.; Camillone, N.; White, M. G. Electronic Structure of the Thiophene/Au(111) Interface Probed by Two-Photon Photoemission. *J. Phys. Chem. C* **2010**, *114*, 13670–13677.
18. Di Castro, V.; Bussolotti, F.; Mariani, C. The Evolution of Benzenethiol Self-Assembled Monolayer on the Cu(100) Surface. *Surf. Sci.* **2005**, *598*, 218–225.
19. Lindsay, S. M.; Ratner, M. A. Molecular Transport Junctions: Clearing Mists. *Adv. Mater.* **2007**, *19*, 23–31.
20. Bock, C.; Pham, D. V.; Kunze, U.; Kafer, D.; Witte, G.; Woll, C. Improved Morphology and Charge Carrier Injection in Pentacene Field-Effect Transistors with Thiol-Treated Electrodes. *J. Appl. Phys.* **2006**, *100*, 114517–7.
21. Jiang, P.; Deng, K.; Fichou, D.; Xie, S.-S.; Nion, A.; Wang, C. STM Imaging *ortho*- and *para*-Fluorothiophenol Self-Assembled Monolayers on Au(111). *Langmuir* **2009**, *25*, 5012–5017.
22. Kwon, K.-Y.; Pawin, G.; Wong, K. L.; Peters, E.; Kim, D.; Hong, S.; Rahman, T. S.; Marsella, M.; Bartels, L. H-Atom Position as Pattern-Determining Factor in Arenethiol Films. *J. Am. Chem. Soc.* **2009**, *131*, 5540–5545.
23. Wong, K. L.; Lin, X.; Kwon, K. Y.; Pawin, G.; Rao, B. V.; Liu, A.; Bartels, L.; Stolbov, S.; Rahman, T. S. Halogen-Substituted Thiophenol Molecules on Cu(111). *Langmuir* **2004**, *20*, 10928–10934.
24. Agron, P. A.; Carlson, T. A. Angular Resolved UPS and XPS Spectra of Benzenethiol Adsorbed on Cu(111) at 300K. *J. Vac. Sci. Technol.* **1982**, *20*, 815–817.
25. Schmidt, C.; Witt, A.; Witte, G. Tailoring the Cu(100) Work Function by Substituted Benzenethiolate Self-Assembled Monolayers. *J. Phys. Chem. A* **2011**, *115*, 7234–7241.
26. Hengsberger, M.; Baumberger, F.; Neff, H. J.; Greber, T.; Osterwalder, J. Photoemission Momentum Mapping and Wave Function Analysis of Surface and Bulk States on Flat Cu(111) and Stepped Cu(443) Surfaces: A Two-Photon Photoemission Study. *Phys. Rev. B* **2008**, *77*, 085425.
27. Lobo-Checa, J.; Matena, M.; Müller, K.; Dil, J. H.; Meier, F.; Gade, L. H.; Jung, T. A.; Stöhr, M. Band Formation from Coupled Quantum Dots Formed by a Nanoporous Network on a Copper Surface. *Science* **2009**, *325*, 300–303.
28. Vondrak, T.; Wang, H.; Winget, P.; Cramer, C. J.; Zhu, X. Y. Interfacial Electronic Structure in Thiolate Self-Assembled Monolayers: Implication for Molecular Electronics. *J. Am. Chem. Soc.* **2000**, *122*, 4700–4707.
29. Föhlisch, A.; Feulner, P.; Hennies, F.; Fink, A.; Menzel, D.; Sanchez-Portal, D.; Echenique, P.; Wurth, W. Direct Observation of Electron Dynamics in the Attosecond Domain. *Nature* **2005**, *436*, 373–376.
30. Nakaya, M.; Shikishima, M.; Shibuta, M.; Hirata, N.; Eguchi, T.; Nakajima, A. Molecular-Scale and Wide-Energy-Range Tunneling Spectroscopy on Self-Assembled Monolayers of Alkanethiol Molecules. *ACS Nano* **2012**, *6*, 8728–8734.
31. Leschik, G.; Courths, R.; Wern, H. Electronic Structure Investigation of Cu(001)-p(2 $\times$ 2) S Using Angle-Resolved

Photoemission and Inverse Photoemission. *Surf. Sci.* **1993**, *294*, 355–366.
32. Muntwiler, M.; Lindstrom, C. D.; Zhu, X. Y. Delocalized Electron Resonance at the Alkanethiolate Self-Assembled Monolayer/Au(111) Interface. *J. Chem. Phys.* **2006**, *124*, 081104.
33. Bussolotti, F.; Corradini, V.; Di Castro, V.; Grazia Betti, M.; Mariani, C. Electronic Structure of Methanethiolate Self-Assembled on the Cu (100) Surface. *Surf. Sci.* **2004**, *566*, 591–596.
34. Driver, S. M.; Woodruff, D. P. Scanning Tunnelling Microscopy Study of the Interaction of Dimethyl Disulphide with Cu(111). *Surf. Sci.* **2000**, *457*, 11–23.
35. Driver, S. M.; Woodruff, D. P. Adsorption Structures of 1-Octanethiol on Cu(111) Studied by Scanning Tunneling Microscopy. *Langmuir* **2000**, *16*, 6693–6700.
36. Perebeinos, V.; Newton, M. Electronic Structure of $S-C_6H_5$ Self-Assembled Monolayers on Cu(111) and Au(111) Substrates. *Chem. Phys.* **2005**, *319*, 159–166.
37. Schmidt, C.; Götzen, J.; Witte, G. Temporal Evolution of Benzenethiolate SAMs on Cu(100). *Langmuir* **2011**, *27*, 1025–1032.
38. Dougherty, D. B.; Maksymovych, P.; Lee, J.; Yates, J. T., Jr. Local Spectroscopy of Image-Potential-Derived States: From Single Molecules to Monolayers of Benzene on Cu(111). *Phys. Rev. Lett.* **2006**, *97*, 236806.
39. Munakata, T.; Sakashita, T.; Shudo, K.-i. Two-Photon Photoemission from Benzene Adsorbed on Cu(111). *J. Electron Spectrosc. Relat. Phenom.* **1998**, *88−91*, 591–595.
40. Velic, D.; Hotzel, A.; Wolf, M.; Ertl, G. Electronic States of the C_6H_6/Cu 111 System: Energetics, Femtosecond Dynamics, and Adsorption Morphology. *J. Chem. Phys.* **1998**, *109*, 9155–9165.
41. Ziroff, J.; Gold, P.; Bendounan, A.; Forster, F.; Reinert, F. Adsorption Energy and Geometry of Physisorbed Organic Molecules on Au(111) Probed by Surface-State Photoemission. *Surf. Sci.* **2009**, *603*, 354–358.
42. Schwalb, C. H.; Sachs, S.; Marks, M.; Schöll, A.; Reinert, F.; Umbach, E.; Höfer, U. Electron Lifetime in a Shockley-Type Metal−Organic Interface State. *Phys. Rev. Lett.* **2008**, *101*, 146801.
43. Muller, E. A.; Johns, J. E.; Caplins, B. W.; Harris, C. B. Quantum Confinement and Anisotropy in Thin-Film Molecular Semiconductors. *Phys. Rev. B* **2011**, *83*, 165422.
44. Cahen, D.; Kahn, A. Electron Energetics at Surfaces and Interfaces: Concepts and Experiments. *Adv. Mater.* **2003**, *15*, 271–277.
45. Alloway, D. M.; Hofmann, M.; Smith, D. L.; Gruhn, N. E.; Graham, A. L.; Colorado, R.; Wysocki, V. H.; Lee, T. R.; Lee, P. A.; Armstrong, N. R. Interface Dipoles Arising from Self-Assembled Monolayers on Gold: UV−Photoemission Studies of Alkanethiols and Partially Fluorinated Alkanethiols. *J. Phys. Chem. B* **2003**, *107*, 11690–11699.
46. Li, H.; Duan, Y.; Paramonov, P.; Coropceanu, V.; Brédas, J.-L. Electronic Structure of Self-Assembled Fluoromethylthiol Monolayers on the Au(111) Surface: Impact of Fluorination and Coverage Density. *J. Electron Spectrosc. Relat. Phenom.* **2009**, *174*, 70–77.
47. Romaner, L.; Heimel, G.; Zojer, E. Electronic Structure of Thiol-Bonded Self-Assembled Monolayers: Impact of Coverage. *Phys. Rev. B* **2008**, *77*, 045113.
48. Whelan, C. M.; Barnes, C. J.; Walker, C. G. H.; Brown, N. M. D. Benzenethiol Adsorption on Au(111) Studied by Synchrotron ARUPS, HREELS, and XPS. *Surf. Sci.* **1999**, *425*, 195–211.
49. Kim, B.; Choi, S. H.; Zhu, X. Y.; Frisbie, C. D. Molecular Tunnel Junctions Based on π-Conjugated Oligoacene Thiols and Dithiols between Ag, Au, and Pt Contacts: Effect of Surface Linking Group and Metal Work Function. *J. Am. Chem. Soc.* **2011**, *133*, 19864–19877.
50. Pasquali, L.; Terzi, F.; Seeber, R.; Doyle, B. P.; Nannarone, S. Adsorption Geometry Variation of 1,4-Benzenedimethanethiol Self-Assembled Monolayers on Au(111) Grown from the Vapor Phase. *J. Chem. Phys.* **2008**, *128*, 134711–10.
51. Rieley, H.; Price, N. J.; White, R. G.; Blyth, R. I. R.; Robinson, A. W. A NEXAFS and UPS Study of Thiol Monolayers Self-Assembled on Gold. *Surf. Sci.* **1995**, 331–333; *Part A*189–195.
52. Wang, S. C.; Yilmaz, M. B.; Knox, K. R.; Zaki, N.; Dadap, J. I.; Valla, T.; Johnson, P. D.; Osgood, R. M., Jr. Electronic Structure of a Co-Decorated Vicinal Cu(775) Surface: High-Resolution Photoemission Spectroscopy. *Phys. Rev. B* **2008**, *77*, 115448.
53. Bertel, E.; Lehmann, J. Electronic Structure of Self-Organized Lateral Superlattices on a Metal Surface: O/Cu(110). *Phys. Rev. Lett.* **1998**, *80*, 1497–1500.
54. Hörmandinger, G.; Pendry, J. B. Interaction of Surface States with Rows of Adsorbed Atoms and Other One-Dimensional Scatterers. *Phys. Rev. B* **1994**, *50*, 18607–18620.
55. Baumberger, F.; Greber, T.; Delley, B.; Osterwalder, J. Tailoring Confining Barriers for Surface States by Step Decoration: CO/Vicinal Cu(111). *Phys. Rev. Lett.* **2002**, *88*, 237601.